Received: 1 November 2022 | Revised: 27 January 2023 | Accepted: 29 January 2023

DOI: 10.1111/ijac.14368

International Journal of Applied Ceramic Technology

RESEARCH ARTICLE

Sintering behavior of 8YSZ-Ni cermet: Comparison between conventional, FST/SPS, and flash sintering

Raghav Mundra[1] | **Tarini Prasad Mishra**[2] | **Martin Bram**[2] | **Olivier Guillon**[2,3] | **Devinder Yadav**[1]

[1]Department of Metallurgical and Materials Engineering, Indian Institute of Technology Patna, Bihta, India

[2]Institute of Energy and Climate Research, IEK-1: Materials Synthesis and Processing, Forschungszentrum Jülich GmbH, Jülich, Germany

[3]Institute of Mineral Engineering (GHI), RWTH Aachen University, Germany

Correspondence
Devinder Yadav, Department of Metallurgical and Materials Engineering, Indian Institute of Technology Patna, Bihta, Patna, India.
Email: devinder@iitp.ac.in

Olivier Guillon, Institute of Energy and Climate Research, IEK-1: Materials Synthesis and Processing, Forschungszentrum Jülich GmbH, Jülich, Germany.
Email: o.guillon@fz-juelich.de

Funding information
Science and Engineering Research Board, Grant/Award Number: SRG/2019/000829; Manipulation of Matter Controlled by Electric and Magnetic Fields: Toward Novel Synthesis and Processing Routes of Inorganic Materials, Grant/Award Number: Fileds Matter SPP 1959; Deutscher Akademischer Austauschdienst, Grant/Award Number: KOSPIE 91755018

Abstract

Cermets are ceramic metal composites. The metallic phase in the cermet typically undergoes oxidation during sintering in air. Electric field-assisted sintering processes such as field-assisted sintering technology/spark plasma sintering (FAST/SPS) and flash involves very high heating rates, short processing time and low processing temperature. The main aim of this work was to see if field-assisted sintering techniques can prevent the oxidation of the metallic phase in the cermet. Sintering behavior of 8YSZ-5 wt.% Ni cermet was studied by three different techniques namely; conventional sintering, FAST/SPS and flash sintering. Phases and microstructure were analyzed through X-ray diffraction and scanning electron microscopy, respectively. Temperature and time required for sintering the samples via FAST/SPS and flash sintering was significantly lower than that during conventional sintering. In addition, we found limited grain growth during FAST/SPS and flash sintering. During conventional sintering in reducing atmosphere (Ar and vacuum), Ni particles retained their elemental state, however the extent of densification was poor in the cermet. FAST/SPS in argon and vacuum resulted in almost complete densification (relative density > 97%) and Ni particles were retained in their elemental state in the cermet. During flash sintering in air, the samples sintered to a high densification (relative density ~98%), however, Ni particles were completely oxidized.

KEYWORDS
ceramic-metal systems, field assisted sintering technology (FAST), sinter/sintering

1 | INTRODUCTION

Cermets are composite materials of ceramics and metals. Cermets combine properties of ceramic such as high hardness, wear resistance and compressive strength with good ductility and fracture toughness of metals.[1,2] Cermets are generally processed by sintering the powder mixture of ceramic and metal. Conventional sintering is performed by heating the—optional net-shaped—green bodies to high temperature for prolonged time.[3,4] Oxidation of the metallic phase occur during sintering of the cermet in air which often leads to a drop in mechanical properties

and corrosion resistance of the cermet. This can be prevented by sintering in reducing atmosphere. However, now the extent of densification of the ceramic phase may be affected. 8 mol.% yttria stabilized zirconia (8YSZ) is one of the most studied material for electric field assisted sintering processes. 8YSZ is a good ionic conductor and possess good chemical and thermal stability.[5] 8YSZ-Ni cermets are used as anode material of solid oxide fuel cells (SOFCs). Ni as a metallic phase in the cermet has two functions. On the one hand it catalyses the oxidation of hydrogen, on the other hand it helps to provide a conductive path, thus increasing the electronic-ionic conductivity. 8YSZ-Ni cermets are conventionally fabricated by sintering mixture of 8YSZ and NiO under oxidising conditions in air. Immediately before operation of the cell, NiO is reduced[6] to Ni by feeding reducing gas (e.g., hydrogen) through the respective gas manifold. This step also leads to a significant increase of the porosity. Dickey et al.[7] showed that during reduction of NiO, the oxygen ions move through YSZ lattice. If during SOFC operation air enters the anode manifold, re-oxidation of Ni increase its volume (by 71.2 %), which can lead to development of stresses in the cermet[8] and can result in formation of cracks.[9] This effect degrades the performance of the cell. If during processing of 8YSZ-Ni cermets in air the oxidation of Ni can be prevented by high heating rates, then the processed cermet can be directly used in the SOFCs without undergoing the need of additional step of reduction.

Application of electric fields adds flexibility to the sintering process and offers fundamentally new materials processing conditions to obtain materials with unique properties.[10,11] Field-assisted sintering techniques such as field-assisted sintering technology/spark plasma sintering (FAST/SPS)[12] and flash sintering[13] involves high sample heating rates and can reduce the time and temperature for a given sintering cycle.[14] In most of the cases, samples are sintered to a high relative density with very minimal grain growth. The FAST/SPS process involves application of low voltage electric pulses of high current along with uniaxial pressure onto the green body.[15] The green body is generally placed inside an electrically conducting die, mostly made of graphite. A controlled atmosphere—usually vacuum or Argon to protect the graphite from oxidation—is maintained inside the setup.[16] During FAST/SPS of ceramic materials such as 8YSZ, rapid heating is caused by the effective Joule heating of the tool and the direct heat transfer from the die to the sample by thermal conduction. On the other hand, flash sintering is a pressureless sintering technique where electric field is applied across the sample via two electrodes and the current entirely passes through the sample, at very low furnace temperature. Flash sintering phenomena is primarily characterized by a nonlinear rise in the conductivity of the sample. The sample densifies in few seconds and exhibits luminescence.[17] Several phenomena associated with the electric current, including; Joule heating,[14] softening,[18] electromigration,[19] electroplasticity,[20] and defect generation[21] are reported to occur in the materials.

The objectives of this work involve studying the sintering behavior of a cermet powder mixture (8YSZ-5Ni) by different techniques, enabling high heating rates. We chose 8YSZ-Ni cermet as it is widely used in SOFCs. In the present work we chose 5 wt.% Ni to stay clearly below the percolation limit for enabling safe flash sintering. The main focus of this study is to probe if oxidation of the metal phase—in the present case Ni—can be reliably avoided in the cermet by sintering with high heating rates. In the case of proving this hypothesis, main findings of the study are the basis for transferring the results to other cermet compositions. Variety of materials have been sintered through electric field-assisted sintering processes; however, a comparative study has not been performed, especially on cermets in different atmospheres.

2 | EXPERIMENTAL PROCEDURES

2.1 | Materials

Powders of 8YSZ (TZ-8Y) were procured from Tosoh Corporation having specific surface area of 14.216 m^2/g and a theoretical density of 5.997 g/cm^3. The average particle size (d_{50}) was 155 nm. Nickel powder (T123TM Nickle powder (CDN), Vale, France) with specific surface area of .436 m^2/g was used as the metallic phase. The theoretical density of nickel was 8.905 g/cm^3, and the average particle size (d_{50}) was 9.4 μm. Powders of 8YSZ and Ni (5 wt.% [3.43 vol.%]) were mixed in a mortar and pestle. Theoretical density of the mixture was calculated by the rule of mixture. For density calculation of samples with oxidised Ni, complete oxidation of Ni was assumed.

2.2 | Sample processing and characterization

2.2.1 | Conventional sintering

The powder mixtures were cold pressed into cylindrical pellets having diameter of 20 mm and thickness of around 5 mm with an applied pressure of 70 MPa. The relative density of the green pellets was ~43%. Conventional sintering of 8YSZ-5Ni pellets in air was carried out in a chamber furnace (Therm-Aix, Type 1810, Aachen, Germany). Conventional sintering of 8YSZ-5Ni pellets in vacuum and argon was carried out in a vacuum furnace (HTK25 Mo/16-1G, Gero, Neuhausen, Germany). In the

case of vacuum operation, the oxygen partial pressure was below 10^{-4} mbar. In the case of operation with argon, the chamber was first evacuated and then flooded with Ar 5.0 (purity 99.999%). For all sintering atmospheres, the samples were heated to a temperature of 1400°C for 2 h. The heating and cooling rate was set to 3°C/min. The temperature was chosen to stay below the melting point of Ni.

2.2.2 | FAST/SPS

FAST/SPS was performed in a FAST/SPS device (HP-D5, FCT System, Rauenstein, Germany). The powder mixture (6 g) was placed in a cylindrical graphite die of 20 mm diameter (Graphite from SGL Carbon GmbH, Germany. Grade SIGRAFINE R7710). A graphite foil was used to improve the contact between the punches and the sample and also between the punches and the die. The thickness of the graphite foil (SGL Carbon GmbH, SIGRAFEX, grade E) was .37 mm. The outer side of the graphite die was covered with soft graphite felt (SGL Carbon GmbH, SIGRATHERM felt, grade GFA 10) for thermal insulation. A constant uniaxial pressure of 50 MPa was applied during the entire temperature cycle. The hydraulic force acted on the lower punch. The heating rate was set to 100°C/min. The FAST/SPS of 8YSZ-5Ni samples was performed at 1300°C in two different atmospheres; vacuum and argon. In the case of vacuum operation, the oxygen partial pressure was approximately .5 mbar. In the case of operation with argon, the chamber was first evacuated and then flooded with Ar 5.0 (purity 99.999%). The samples were held at the maximum temperature for 10 min. The temperature during FAST/SPS cycles was measured by a vertical pyrometer enabling to measure temperatures starting from 400°C. To ensure temperature measurement near to the sample, a ∅ 10 mm hole was drilled in the upper punch and the temperature was measured at the bottom of the hole. The distance between the bottom and the upper face of the sample was 5 mm.

2.2.3 | Flash sintering

For flash sintering experiments, the powders were compacted at an applied pressure of 70 MPa into dog-bone shaped specimen having holes at its ends. The gage length, breadth and thickness was 15, 3.5, and 1.58 mm, respectively. The relative density of the green samples was around 45%. The samples were hung into a horizontal split tubular furnace (Applied Test Systems, USA) with the help of platinum wires, which also acted as electrodes for applying electric field. Platinum paste was applied in the vicinity of the holes for better electrical contact. A DC power source (DLM300-2 Sorensen) was used for applying the electric field across the sample and for passing the current. The current flowing through the sample was measured by a digital multimeter (Keithley 2000) connected in series with the circuit. The sample shrinkage was measured though a monochrome camera, placed in front of the furnace. The electrical parameters were controlled through Matlab program. Isothermal flash sintering experiments were performed in air at a furnace temperature of 850°C. The samples were held at the temperature for 15 min to ensure uniform temperature across the sample. Then, an electric field of 100 V/cm was applied across the sample. The maximum current density was set to 120 mA/mm^2. After onset of flash, the samples were held at the constant current value for 35 s before turning off the power supply. In the state of flash, the sample temperature rises significantly above the furnace temperature. The sample surface temperature in the state of flash was measured with a micro-epsilon laser pyrometer. The sample temperature was also estimated by the black body radiation (BBR) model.

2.3 | Sample characterization

Theoretical density measurements of the powders were performed using Ultrapyc 1200e (Quantachrome Instruments) single station automatic gas pycnometer operating in nitrogen atmosphere. The relative density of the sintered samples was calculated by the Archimedes method. Particle size distribution (d_{50}) measurement was performed by laser diffraction with LA-950V2 (Hoiba/Retsch). The specific surface area of both the powders was calculated using AREA-mat (Jung Instrument, GmbH) surface area analyser. X-ray diffraction (XRD) was performed in a Bruker-AXS/D4 Endeavor diffractometer using Cu target ($\lambda = 1.5481$ Å) with step size of .02° and time per step of .75 s/step. XRD data were analyzed through TOPAS software (Bruker AXS). The sintered samples were metallographically polished. The samples were then subjected to thermal etching by heating the samples to a temperature 150°C less than their respective sintering temperature in the same atmosphere in which they were sintered, for 20 min. The microstructural studies were performed in a Zeiss "Ultra55" field emission gun scanning electron microscope equipped with an energy dispersive spectroscopy (EDS)-system of the Oxford Instruments (detector type: X-max 80 mm^2, software: INCAEnergy400). The samples were coated with a thin film of platinum before the SEM analysis. Average grain size was calculated by the linear intercept method using Image J software. Only 8YSZ phase was considered.

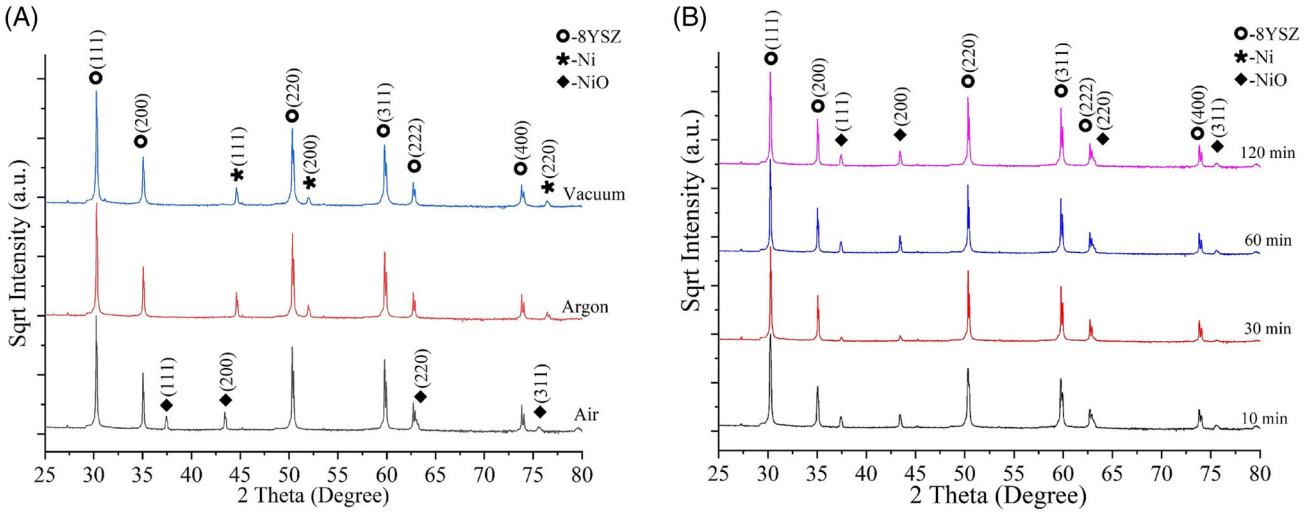

FIGURE 1 X-ray diffraction (XRD) patterns of conventionally sintered 8YSZ-5Ni pellets (A) in different atmospheres at 1400°C-2 h and (B) sintered at 1400°C in air at different hold times.

3 | RESULTS

3.1 | Conventional sintering of 8YSZ-5Ni green compact

The cermet powder mixture was conventionally sintered at 1400°C for 2 h in three different atmospheres; air, argon, and vacuum. The XRD pattern of conventionally sintered 8YSZ-5Ni sample in different sintering atmospheres is shown in Figure 1A. In air, Ni transformed to NiO, while it remained in its elemental state in argon and vacuum. There was no sign of any residual Ni phase after conventional sintering in air, indicating complete oxidation of Ni in the cermet, turning it into an 8YSZ-NiO composite. When conventionally sintering in air, the pellets sintered to a high relative density (~97.2%) and the samples had a greenish appearance indicating the oxidation of Ni. The samples sintered in vacuum and argon had greyish appearance. The relative density was calculated assuming complete oxidation of Ni. To know what occurs first, oxidation of Ni or densification, the cermet was conventionally sintered at 1400°C using different hold times, namely, 10, 30, 60, and 120 min. The XRD patterns of these samples are given in Figure 1B. It can be seen that Ni transformed to NiO even when the holding time was 10 min, at 1400°C. The relative density of the pellet was 87.8% after 10 min of hold time. This clearly shows that the oxidation of Ni occurred before complete sintering of the sample. According to literature,[22,23] Ni oxidation starts at 400–500°C. The oxidation rate is reported to be sub-parabolic (decrease rapidly with time) in the temperature range of 700–1000°C and parabolic (weight gain $\propto \sqrt{t}$) in the temperature range of 1100–1400°C.

The microstructure of the samples sintered in different environments is shown in Figure 2A–C. The relative density and the average grain size of the 8YSZ phase is given in Table 1. It can be seen that the extent of densification was higher in air, followed by vacuum and then in argon. The average grain size was not calculated for the samples sintered in reducing atmosphere as the sample density was too low. The EDS point analysis on the particles confirmed them to be NiO when sintered in air and in their elemental state when sintered in argon and vacuum. The EDS results are given in the supplementary file (Figure S1a and b).

For the conventionally sintered samples, the extent of densification was less in argon atmosphere and vacuum compared to, in air. It is worth mentioning here that for SOFC applications, high porosity is required; however for structural applications high density cermet is desired. Sintering depends on the defect chemistry, type of defect and the mode of mass transport. The slowest moving species control the rate of densification.

When the cermet is sintered in reducing atmosphere, Ni particles are retained in their elemental state. Ni can go into the solid solution of zirconia up to 3 wt.%. Valigi et al.[24] reported that at a temperature of 500°C, Ni ions are incorporated at the substitutional sites into the zirconia lattice forming a solid solution (up to 3 wt.%). The incorporation of Ni on the surface of ZrO_2 particles, hinders the sintering of ZrO_2 particles, thereby slowing down the sintering process in reducing atmosphere. This could be one of the reasons for poor sintering in vacuum and argon atmosphere. In addition, in vacuum since there is no gas flow or no convection to spread the heat there is improper distribution of heat, compared to argon atmosphere.[25] This also limits the densification. Usually much higher

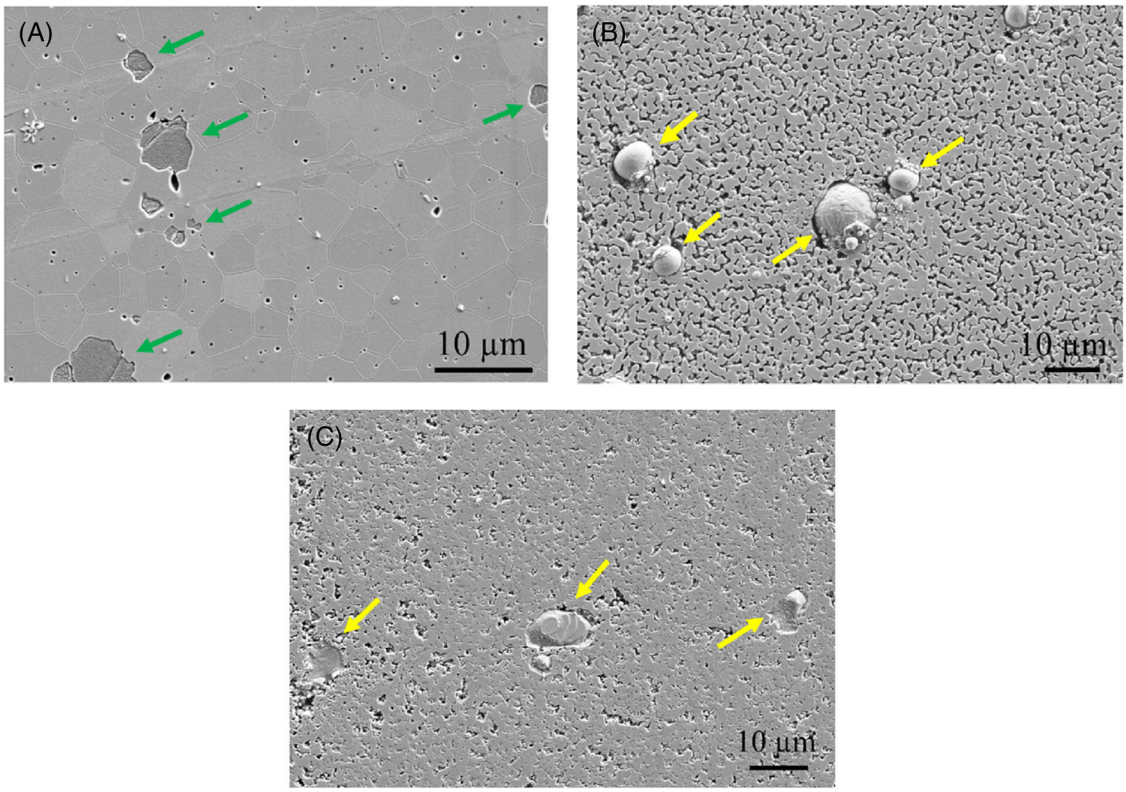

FIGURE 2 SEM images of conventionally sintered 8YSZ-5Ni pellets in (A) air, (B) argon, (C) vacuum at 1400°C for 2 h. NiO (green) and Ni (yellow) particles are marked by arrows. Related EDS measurements are given as Figure S1.

TABLE 1 Relative density and average grain size (8YSZ phase) in the 8YSZ-5Ni cermet, sintered by different techniques

Method	Atmosphere	Relative density (%)	Average grain size (μm)	Phases present
Conventional sintering (1400°C – 2 h)	Air	97.21	3.79	8YSZ and NiO
	Vacuum	75.75		8YSZ and Ni
	Argon	68.58		8YSZ and Ni
FAST/SPS (1300°C)	Vacuum	98.43	1.06	8YSZ and Ni
	Argon	97.48	1.01	8YSZ and Ni
Flash sintering (850°C)	Air	97.6	1.22	8YSZ and NiO

temperatures are required in vacuum to obtain dense ZrO_2-Y_2O_3 ceramics.[26] However, the exact reason for lower densification in vacuum and argon needs to be probed through further experiments.

3.2 | FAST/SPS of 8YSZ-5Ni powder mixture

FAST/SPS of the 8YSZ-5Ni samples was performed in inert (argon) atmosphere and vacuum at 1300°C with 10 min of holding time. The heating rate was kept at 100°C/min. The relative piston movement with respect to time is shown in Figure 3A. It can be seen that the relative piston movement is similar in both the atmospheres, indicating same extent of densification. In the case of argon, the main densification appears at slightly higher temperatures with a ΔT of approximately 20°C (not shown here). The XRD pattern of the sintered samples in Figure 3B shows that during FAST/SPS, Ni retained in its elemental state in argon and vacuum. The samples had a greyish appearance even after removing the graphite layer. The microstructure of the sintered pellets is shown in Figure 3C and D. The relative density and the average grain size are mentioned in Table 1. The extent of densification was better in FAST/SPS than in conventional sintering. In addition, the average grain size of 8YSZ phase was smaller. The heating rates in FAST/SPS are much higher than conventional sintering, in addition

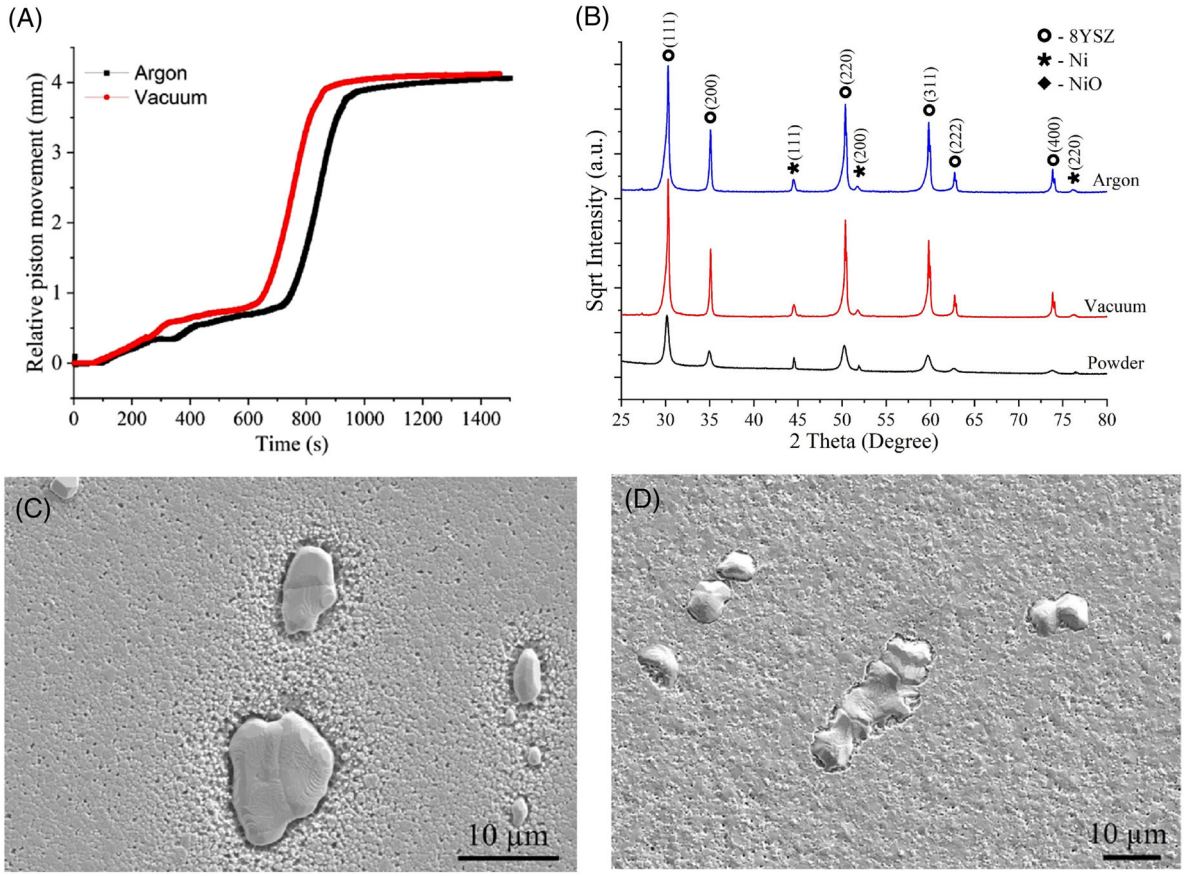

FIGURE 3 (A) Densification curves of spark plasma sintered 8YSZ-5Ni pellets in different atmospheres, (B) X-ray diffraction (XRD) patterns of spark plasma sintered 8YSZ-5Ni pellets in different atmospheres and SEM images of the sintered samples in (C) argon and (D) vacuum.

to the applied pressure. The EDS results of the FAST/SPS samples are given in Figure S2.

In the microstructure of the FAST/SPS samples especially in argon, pores were observed around the nickel particles, showing lower extent of densification in the 8YSZ phase. This is due to the effect of a rigid inclusion (Ni particle/agglomerate), which are dense and therefore induces some tensile stresses in the surrounding YSZ matrix and residual porosity.[27] The ZrO_2 matrix is densifying into rigid Ni particles, applying compressive stress on the particles.

3.3 | Flash sintering of 8YSZ-5Ni green compact

Flash sintering of 8YSZ-5Ni powder mixture was performed in air. The initiation of the flash is followed by a nonlinear rise in the specimen's electrical conductivity. A constant heating rate experiment was performed at an applied electric field of 100 V/cm to know the minimum furnace temperature required for flash sintering. The sample flash sintered at a furnace temperature of 796°C. Isothermal flash sintering experiments were performed at a furnace temperature 50°C higher, that is, at 850°C. The current density limit was set to 120 mA/mm^2. The samples were held in the state of flash (stage III) for 35 s. The total duration of the flash sintering experiment was 50 s. The laser pyrometer recorded the sample surface temperature to be 1190–1200°C in the state of flash (stage III of flash, when constant current flow through the sample). The estimated sample temperature from black body radiation model[28] was around 1340°C in the state of flash. The emissivity was taken to be .9 for the pyrometer and BBR model. It can be seen that the sample temperature estimated by BBR and measured by pyrometer are around 100°C different. The difference in the BBR and the pyrometer temperature points toward an energy deficit.[29] This energy is absorbed within the sample to generate point defects. Hence a part of the power dissipated in the sample is consumed in defect generation and rest is lost in radiation.[29] In addition, the pyrometer measures only the surface temperature of the sample. The radiative and convection heat loss from the surface

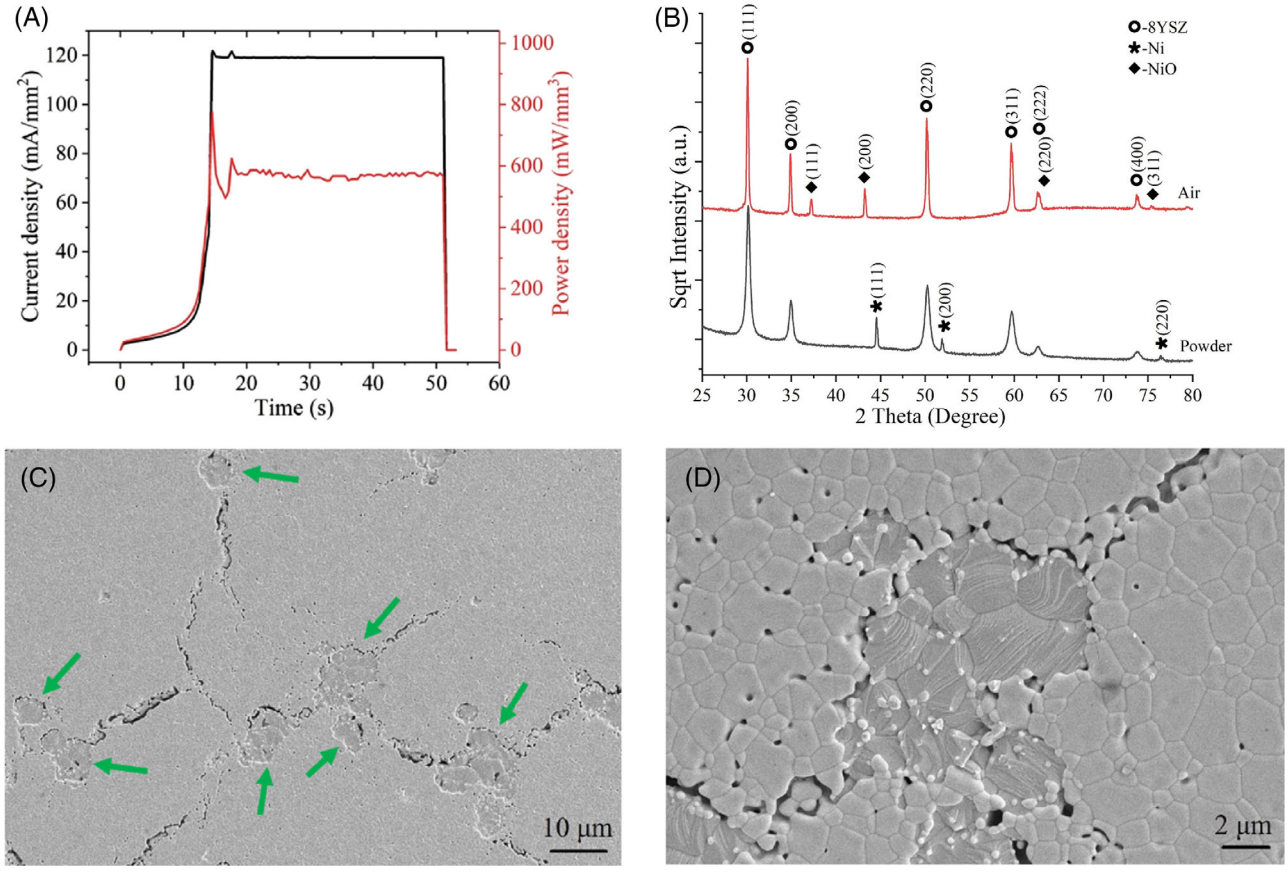

FIGURE 4 (A) Electric parameters during isothermal flash sintering experiment, (B) X-ray diffraction (XRD) pattern of flash sintered 8YSZ-5Ni sample and (C) and (D) SEM images of the microstructure. NiO particles are marked by arrows.

might induce thermal gradient and surface is at lower temperature than the core during flash sintering. This could be another reason for the variation in sample temperature estimated by BBR model and measured by pyrometer. The electrical parameters (current density and the power density) from the flash sintering experiments are plotted in Figure 4A. The XRD pattern of the flash sintered samples showed peaks corresponding to NiO, and no peaks of Ni were observed (Figure 4B). The microstructure of the sintered sample is shown in Figure 4C and D. The samples had greenish appearance due to Ni oxidation. The grain size of NiO was larger than that of 8YSZ phase. The relative density and the average grain size are reported in Table 1. Pores were observed at the interphase between 8YSZ and NiO. Some long interconnected pores were observed, apparently formed by the accumulation of many pores. The EDS results of the flash sintered samples are given in Figure S3. Flash sintering experiments were not performed in reducing atmosphere. Very recently it was reported that flash sintering of 8YSZ in reducing atmosphere resulted in poor densification, compared to air.[30]

4 | DISCUSSION

YSZ and NiO have low wettability, are immiscible, and do not react with each other over a wide range of temperatures.[31] Matsushima et al.[32] reported that the temperature at which sintering begins in 8YSZ, is not affected by NiO content. The authors also reported that the extent of densification reduced as NiO content increased (from 40 wt.% to 60 wt.%) above 1300°C. However, in the present case, the amount of NiO was much smaller, below the percolation threshold. Therefore, it is expected that its influence on the extent of densification of the composite mixture in the composite would be negligible. Presence of NiO would not change the sintering characteristics of 8YSZ.

We can clearly see a reduction in furnace temperature and time when moving from conventional sintering to FAST/SPS and then to flash sintering. This shows the effectiveness of electrical energy in accelerating the diffusion kinetics to densify the cermet faster and at lower temperatures. In ideal case, this could lead to energy savings during manufacturing of cermet, but scaling up of these

technologies is still at the beginning. The applied external fields in the FAST/SPS and flash sintering experiments help in fast firing during sintering. Although the applied electric fields are low in FAST/SPS, current passing through the die is very high. The conductive graphite die transfers the heat to the sample by thermal conduction. In flash sintering, the applied electric fields are relatively high and the total current is low; however, all the current passes through the sample. The three sintering techniques involve different processing conditions, process parameters, and involve different mechanisms of mass transport. However, a simple comparison of the three processes can be performed by comparing the involved sample heating rates. Here, we can incorporate the effect of the electrical parameters (field and current) in terms of sample heating rate. The heating rates affect the sintering behavior of the materials in several ways. The high heating rates enable high sintering ability of the powders. Zhou et al.[33] showed that by increasing the heating rates from 50 to 300°C/min, the sintering time reduced by six times during FAST/SPS of alumina. This indicates that the shrinkage rates are proportional to the heating rates. It is to be noted here that the extent of densification is controlled by the final temperature and not by the heating rate. During conventional sintering, the non-densifying mechanisms (surface diffusion, lattice diffusion from surface, and vapor transport) operate at lower temperature and the densifying mechanisms (grain boundary diffusion, lattice diffusion from grain boundary, and plastic flow) operate at high temperatures. High heating rates are known to strongly limit the non-densifying mechanisms and promote the densifying mechanisms already at lower temperature.[34,35] At early stages of sintering, the surface diffusion is suppressed. This delays the spheroidization of the pore and grain boundary diffusion starts to operate early. The high heating rates in FAST/SPS (100°C/min) and flash sintering (~1000°C/min)[36] increase the driving force for densification of particles and help in suppressing the grain coarsening. During FAST/SPS the applied load also contributes to densification. Wang and Raj[37] reported that the densification rate is inversely proportional to the forth power of the grain size. Hence, a small increase in the grain size will lower the densification rate. The high heating rates in FAST/SPS and flash sintering keeps the grain size small and this in-turn promote high densification rate. In addition, electric field is known to retard the grain growth,[38] thereby retaining the fine-grained structure. It is to be noted here that in Wang and Raj analysis[37] the grain size power depends on the mechanism of diffusion. If the densification rate is controlled by lattice diffusion, $n = 3$ and for grain-boundary diffusion $n = 4$.

The activation energy of Ni oxidation is reported to be 180–240 kJ/mol, which is similar to Ni lattice diffusion at 154–254 kJ/mol.[39] At temperature below 1000°C, NiO growth is dominated by the diffusion of Ni through the grain boundaries of growing NiO and above 1000°C, by lattice diffusion. We observed that Ni particles oxidized when sintered in air, independent if done by conventional sintering or flash sintering. The high heating rates in flash sintering could not prevent the oxidation of Ni in the cermet. From the methods investigated in this study, FAST/SPS appears to be the best technique to obtain dense cermets with fine grain size.

Several athermal effects of electric field are reported to occur during flash sintering. During flash sintering, it is reported that point defects are generated in the material far above the equilibrium value.[21] The high diffusion rates along with high concentration of vacancies can enhance the oxidation rates. It will be interesting to see whether sintering and oxidation occur together, or one predominates the other during flash sintering. Such experiments need to be performed in-situ. The effect of electric field on the kinetics of solid-state phase reaction (oxidation) is an interesting phenomenon and can be studied further. Finally, we would like to mention that the scope of the present study was to investigate if oxidation of the metallic phase (here Ni) in cermets can be avoided by applying high heating rates beyond 100 K/min when conducting sintering in air. For proving this hypothesis, we used a model material (8YSZ – 5 wt.% Ni), which does not have a practical relevance for structural or electrochemical applications.

5 | CONCLUSIONS

In the present work, sintering behavior of 8YSZ-5Ni cermet was studied by three different methods namely, conventional sintering, FAST/SPS and flash sintering. The main aim was to see if oxidation of Ni in the cermet can be prevented by sintering techniques which involved very high heating rates. Below are the specific conclusions.

1. There was a decrease in furnace temperature and time required for full densification of 8YSZ-Ni cermet from conventional sintering to FAST/SPS to flash sintering. The short sintering time will be useful to the industries for faster production.
2. The relative density of the samples sintered conventionally and by flash sintering, in air, was 97.2% and 97.6%, respectively, and the average grain size of 8YSZ phase was 3.8 and 1.2 μm, respectively. For the samples sintered conventionally in vacuum and argon, the relative density was 75.8 and 68.6%, respectively. The relative density of FAST/SPS samples in vacuum and argon was 98.4 and 97.5%, respectively, with the average

grain size of 8YSZ phase being around 1 μm in both the cases.

3. Conventional sintering in reducing atmosphere retained Ni in its elemental state in the cermet; however, the extent of densification was poor. In air, though the densification was good, Ni particles oxidized. The Ni particles were completely oxidized during conventional and flash sintering, when sintering was carried out in air.
4. The high heating rates in flash sintering could not prevent Ni oxidation.
5. Our results reveal that FAST/SPS is the best technique to obtain dense and fine grained 8YSZ-Ni cermet.

AUTHOR CONTRIBUTIONS

Experimentation, analysis, and writing: RM. Design and analysis: TPM. Conceptualization, design, and writing: MB. Funding acquisition, project supervision, and approval: OG. Funding acquisition, project supervision, and writing: DY.

ACKNOWLEDGMENTS

RM wish to express his gratitude to the Deutscher Akademischer Austauschdienst (DAAD), the German Academic Exchange service under the program "Combined Study and Practice Stays for Engineers from Developing Countries (KOSPIE) with Indian IITs, 2019" (ID: 91755018) for providing fellowship to carry out this work. TPM acknowledges the funding received from the German Science Foundation (DFG) under priority program "Fields Matter" (SPP 1959). DY acknowledges the SERB-SRG (grant number: SRG/2019/000829) for the financial support to set up flash sintering facility at IIT Patna. Mr. Pranav Rai acknowledged for his assistance in flash sintering experiments.

Open access funding enabled and organized by Projekt DEAL.

REFERENCES

1. Nicholls J. Advances in coating design for high-performance gas turbines. MRS Bulletin. 2003;28:659–70.
2. Perepezko JH, Bero JM, Sakidja R, Talmy IG, Zaykoski J. Oxidation resistant coatings for refractory metal cermets. Surf Coat Technol. 2012;206:3816–22.
3. Rahaman MN. Ceramic processing and sintering. New York: Marcel Dekker; 1995.
4. Chinelatto ASA, Agnolon EMdJA, de Souza AM, Manosso MK. Mechanisms of microstructure control in conventional sintering. Sintering of ceramics - new emerging techniques. Lakshmanan A, editor. Rijeka, Croatia: Intechopen; 2012:401–22.
5. Badwal S. Zirconia-based solid electrolytes: microstructure, stability and ionic conductivity. Solid State Ionics. 1992:52(1-3):23–32.
6. Menzler NH, Tietz F, Uhlenbruck S, Buchkremer HP, Stöver D. Materials and manufacturing technologies for solid oxide fuel cells. J Mater Sci. 2010;45(12):3109–35.
7. Dickey EC, Dravid VP, Nellist PD, Wallis DJ, Pennycook SJ, Revcolevschi A, Microsc Microanal. 1997;3:443–50.
8. Jeangros Q, Faes A, Wagner JB, Hansen TW, Aschauer U, Van herle J, et al. *In situ* redox cycle of a nickel-YSZ fuel cell anode in an environmental transmission electron microscope. Acta Mat. 2010;58:4578–89.
9. Faes A, Nakajo A, Wyser AH, Dubois D, Brisse A, Modena S, et al. RedOx study of anode-supported solid oxide fuel cell. J Pow Sour. 2009;193:55–64.
10. Olevsky EA, Dudina DV. Field-assisted sintering: science and applications. Cham, Switzerland: Springer; 2019.
11. Orrù R, Licheri R, Locci AM, Cincotti A, Cao G. Consolidation /synthesis of materials by electric current activated/assisted sintering. Mater Sci Eng R. 2009;63(4-6):127–287.
12. Munir ZA, Anselmi-Tamburini U, Ohyanagi M. The effect of electric field and pressure on the synthesis and consolidation of materials: a review of the spark plasma sintering method. J Mater Sci. 2006;41(3):763–77.
13. Biesuz M, Sglavo VM. Flash sintering of ceramics. J Eur Ceram Soc. 2019;39(2-3):115–43.
14. Dancer CEJ. Flash sintering of ceramic materials. Mater Res Exp. 2016;10:102001.
15. Cao G, Estournes C, Garay J, Orrù R. Spark plasma sintering: current status, new developments and challenges: a review of the current trends in SPS. Amsterdam, Netherlands: Elsevier; 2019.
16. Guillon O, Gonzalez-Julian J, Dargatz B, Kessel T, Schierning G, Räthel J, et al. Field-assisted sintering technology/spark plasma sintering: mechanisms, materials, and technology developments. Adv Eng Mater. 2014;16(7):830–49.
17. Cologna M, Rashkova B, Raj R. Flash sintering of nanograin zirconia in <5 s at 850°C. J Am Ceram Soc. 2010;93(11):3556–59.
18. Raj R, Cologna M, Francis JS. Influence of externally imposed and internally generated electrical fields on Grain growth, Diffusional creep, sintering and related phenomena in ceramics. J Am Ceram Soc. 2011;94(7):1941–65.
19. Biesuz M, Pinter L, Saunders T, Reece M, Binner J, Sglavo VM, et al. Investigation of electrochemical, optical and thermal effects during flash sintering of 8YSZ. Materials (Basel). 2018;11(7):1214.
20. Conrad H, Yan D. Influence of an applied DC electric field on the plastic deformation kinetics of Oxide Ceramics. Phil Mag. 2010;90(9):1141–57.
21. Kathiria R, Wolf DE, Raj R, Jongmanns M. Frenkel pairs cause elastic softening in zirconia: theory and experiments. New J Phys. 2021;23(5):053013.
22. Haugsrud R. On the high-temperature oxidation of nickel. Corrosion Sci. 2003;45:211–35.
23. Mrowec S, Grzesik Z. Oxidation of nickel and transport properties of nickel oxide. J Phy Chem Solids. 2004;65:1651–57.
24. Valigi M, Gazzoli D, Dragone R, Gherardi M, Minelli G. Nickel oxide-zirconium oxide: Ni^{2+} incorporation and its influence on the phase transition and sintering of zirconia. J Mater Chem. 1995;5(1):183–9.
25. Li T. Powder injection molding of metallic parts and structures. Encycl Mater Metals alloys. 2022;4:401–16.

26. Sablina TY, Savchenko NL, Mel'nikov AG, Kul'kov SN. Vacuum sintering of a ceramic based on zirconium dioxide. Glass Ceram. 1994;51:198–201.
27. Green DJ, Guillon O, Rödel J. Constrained sintering: a delicate balance of scales. J Eur Ceram Soc. 2008;28:1451–66.
28. Raj R. Joule heating during flash-sintering. J Eur Ceram Soc. 2012;32(10):2293–01.
29. Mishra TP, Neto RRI, Raj R, Guillon O, Bram M. Current-rate flash sintering of gadolinium doped ceria: microstructure and defect generation. Acta Mater. 2020;189:145–53.
30. Bhandari S, Mishra TP, Guillon O, Yadav D, Bram M. Accessing the role of Joule heating on densification during flash sintering of YSZ. Scripta Mater. 2022;211:114508.
31. Park K, Kim J. Effect of Nb_2O_5 content and sintering temperature on the microstructure and bending strength of porous Ni-YSZ Cermets. Ceram Int. 2017;43(2):1740–46.
32. Matsushima T. Effects of sinterability of YSZ powder and NiO content on characteristics of Ni-YSZ cermets. Solid State Ionics. 1998;111(3-4):315–21.
33. Zhou Y, Hirao K, Yamauchi Y, Kanzaki S. Effects of heating rate and particle size on pulse electric current sintering of alumina. Scripta Mater. 2003;48(12):1631–36.
34. Eqbal A, Arya KS, Chakrabarti T. In-depth study of the evolving thermal runaway and thermal gradient in the dog bone sample during flash sintering using finite element analysis. Ceram Int. 2020;46(8):10370–78.
35. Harmer MP, Brook RJ. Fast firing: microstructural benefits, J Br Ceram Soc. 1981;80:147–48.
36. Mostaghaci H, Brook RJ. Production of dense and fine grain size $BaTiO_3$ by fast firing. Trans J Br Ceram Soc. 1983;82:167–69.
37. Wang J, Raj R. Estimate of the activation energies for boundary diffusion from rate-controlled sintering of pure alumina, and alumina doped with zirconia or titania. J Am Ceram Soc. 1990;73(5):1172–75.
38. Ghosh S, Chokshi AH, Lee P, Raj R. A huge effect of weak DC electrical fields on grain growth in zirconia. J Am Ceram Soc. 2009; 92(8):1856–59.
39. Hou PY, Oxidation of nickel, cobalt, and iron (1.10.2): in oxidation of metals and alloys. Shreir's Corrosion. 2010;1:195–239.

SUPPORTING INFORMATION

Additional supporting information can be found online in the Supporting Information section at the end of this article.

How to cite this article: Mundra R, Mishra TP, Bram M, Guillon O, Yadav D. Sintering behavior of 8YSZ-Ni cermet: Comparison between conventional, FST/SPS, and flash sintering. Int J Appl Ceram Technol. 2023;20:2271–2280. https://doi.org/10.1111/ijac.14368